In Vivo Compressed Sensing fMRI using Conventional Gradient-recalled Echo and EPI Sequences

Xiaopeng Zong[1], Juyoung Lee[2], Alexander Poplawsky[3], Seong-Gi Kim[3,4], and Jong Chul Ye[2]

[1]*Biomedical Research Imaging Center, University of North Carolina at Chapel Hill, Chapel Hill, NC, United States,* [2]*Korea Advanced Institute of Science & Technology, Daejon, Korea,* [3]*University of Pittsburgh, PA, United States,* [4]*Dept. of Biological Sciences, SKKU, Suwon, Korea*

Target audience: Researchers interested in functional MRI, accelerated data acquisition, and compressed sensing.

Purpose: Compressed sensing (CS) may be useful for accelerating data acquisitions in high-resolution fMRI. However, due to the inherent slow temporal dynamics of the hemodynamic signals and concerns of potential statistical power loss, the CS approach for fMRI (CS-fMRI) has not been extensively investigated. Most of the existing CS-fMRI studies have been conducted with synthesized experiments where fully sampled k-space data were retrospectively down-sampled, partially because of the difficulty in implementing accelerated fMRI pulse sequences that are free of artifact [1]. However, it is difficult to determine pulse sequence-dependent artifacts as well as potential advantages of improved temporal resolutions using retrospective analyses. Therefore, to verify the usefulness of CS for fMRI, systematic studies using real k-space undersampling sequences must be conducted. We systematically investigated the properties of CS-fMRI using computer simulations and *in vivo* experiments of rat forepaw sensory and odor stimulations with 2-dimensional gradient-recalled echo (GRE) and echo planar imaging (EPI) sequences. K-t FOCUSS with Karhunen-Loeve transform that exploits the temporal redundancy of fMRI images was used to reconstruct the images [2].

Methods: The usefulness of CS fMRI may depend on the pulse sequence, activation spatial extent relative to the imaged area, hemodynamic response function, paradigm design, undersampling scheme, and contrast to noise ratio. Thus, we chose two stimulation conditions (a focal activation site in the primary somatosensory cortex (S1) during forepaw stimulation and large, broader activation regions in the olfactory bulb (OB) during odor stimulation), two fMRI contrasts (positive BOLD in S1 and negative CBV-weighted signal in OB), two paradigms (block-designed and rapid ER), two pulse sequences (GRE and EPI), and multiple sampling patterns with the reduction factors (R) of 2 and 4. For the block-designed forepaw stimulation, each scan consisted of 5 stimulation trials, in which each trial consisted of 4 control, 6 stimulation, and 20 control fully-sampled images with a TR of 1.92 s. For the rapid ER forepaw stimulation, each scan consisted of 150 fully-sampled images, and two stimuli frequencies (3Hz and 8 Hz) were each randomly presented during 20 out of the 150 images. For the block-designed OB stimulation, one scan consisted of 15 control, 8 stimulation, and 15 control fully-sampled images with a TR of 8 s. For the rapid ER OB stimulation, each scan consisted of 38 fully-sampled images, and the two odors of 8-s duration were each randomly presented during 5 out of the 38 image periods. For undersampled data, the number of images was increased by a factor of R while the stimulation pattern remained the same. Three undersampling patterns in k_y (k component along the phase encoding direction) were studied: 1) a "Gaussian" pattern which always samples the $k_y = 0$ line and randomly samples the remaining lines according to a Gaussian probability distribution; 2) a "Rand+C6" pattern which always samples six central k_y lines and randomly selects the remaining lines; 3) a "Rand" pattern which randomly sample k_y with a constant probability over all k_y. In simulation, fMRI data were synthesized by modulating the signal intensity with a canonical hemodynamic response function in predefined regions of the images similar to the activated regions observed in real experiments. Gaussian white noise with different amplitudes were added to the k-space data such that 5 contrast to noise ratios (CNR) of 0.3, 0.5, 1.0, 1.5, and 2.0 were obtained. A general linear model analysis was carried out to determine activated voxels. Receiver operating curves (ROC) of true positive rate versus false positive rate were obtained and the areas under the curves were used as an index for comparing difference sampling patterns. The GRE sequences for OB and S1 studies had an in-plane matrix size of 64×64. Fully sampled 2-shot EPI and undersampled single-shot EPI with R = 2 were also performed for S1 study with an in-plane matrix size of 128×128.

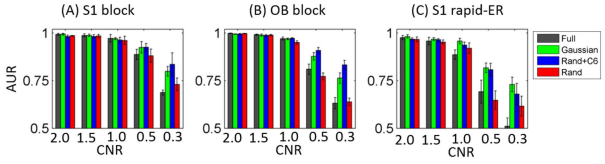

Figure 1: Area under ROC (AUR) versus CNR for 4 sampling patterns in (a) block designed S1, (b) block-designed OB, and (c) rapid ER S1 fMRI studies obtained through simulation. The three undersampled patterns has R = 4.

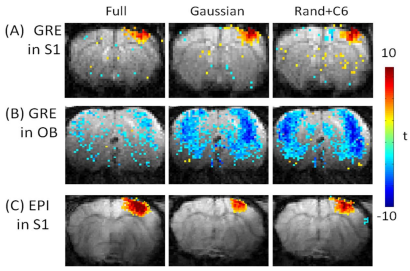

Figure 2: Experimental activation maps in block-designed (a) BOLD fMRI in S1 with GRE and (b) CBV-weighted fMRI with GRE, and (c) BOLD fMRI in S1 with EPI sequence. The Gaussian and Rand+C6 patterns have R = 4 in (a) and (b) and R = 2 in (c).

Results: Figure 1 shows area under ROC versus CNR for the different paradigms and sampling patterns. Performances of the different sampling patterns appear similar at the highest CNR. However, as the CNR decreases, the Gaussian and Rand+C6 patterns provide higher sensitivities than the Rand and full sampling patterns. The AURs for Rand+C6 patterns are either similar to or greater than those for the Gaussian pattern in most cases, suggesting that sampling of several low k_y lines is more beneficial than sampling a single line at k_y=0. Since the Rand+C6 and Gaussian patterns provide better sensitivity in both S1 and OB studies than the Rand pattern, only these two undersampling patterns were used in the actual experiments. No increase of false activation outside the truly activated regions was observed in the activation maps in simulation (data not shown).

Experimental activation maps obtained with the block-designed paradigm are displayed in Fig. 2. Undersampling increases the number of activated voxels with the GRE sequence as demonstrated in Fig. 2A and 2B. However, with the EPI sequence, the sensitivity decreases in the undersampled maps as shown in Fig. 2C. Rapid ER paradigms were also studies with the GRE sequence in S1 and OB, and, similar to the block-designed paradigm, an increase in sensitivity was also observed (data not shown).

Discussion: Our simulation results showed that Gaussian and random sampling with full sampling of some center k-space lines outperform the fully random sampling pattern, although the latter is more incoherent in the KLT transformed domain. Since fMRI signals usually suffer from low SNR and the image contrast is usually determined by the low frequency components, the low frequency samples should be favorably chosen. This is clearly shown in our simulation for the lower SNR cases. Note that most of the high magnitude data points reside around the low k-space region, so the SNR penalty is more significant when skipping k-space data here. Especially, in fMRI, since the SNR loss usually results in statistical sensitivity and specificity losses, a denser sampling at the low frequency range is preferable.

In *in vivo* studies, we found a large increase in sensitivity when applying CS to the GRE sequence, consistent with our simulation results. However, there appears to be no sensitivity gain when CS is applied to the EPI sequence. This difference can be explained by the additional noises introduced by the random sampling in the EPI sequence, which is absent in the GRE sequence.

Conclusions:. Our results show that the improved temporal resolution from CS-fMRI improves the statistical performance of activation detection. We also found that center-weighted random sampling patterns were preferred over the purely random sampling patterns. In summary, our results confirm that CS-fMRI is a viable tool that has great potential to improve the performance of fMRI studies.

References: 1. Jeromin, O., Pattichis, M.S., and Calhoun, V.D., Biomed Eng Online 11, 25 (2012). 2. Jung, H., Sung, K., Nayak, K.S., Kim, E.Y., Ye, J.C., Magn Reson Med 61, 103-116 (2009).